

## ARTICLES

## Solvent Effect on the Deactivation Processes of Benzophenone Ketyl Radicals in the Excited State

Masanori Sakamoto, Xichen Cai, Mamoru Fujitsuka, and Tetsuro Majima\*

*The Institute of Scientific and Industrial Research (SANKEN), Osaka University, Mihogaoka 8-1, Ibaraki, Osaka 567-0047, Japan**Received: January 7, 2006; In Final Form: June 27, 2006*

The solvent effects on ketyl radicals of benzophenone derivatives (BPD) in the excited state ( $\text{BPDH}^*(\text{D}_1)$ ) were investigated. Absorption and fluorescence spectra of  $\text{BPDH}^*(\text{D}_1)$  in various solvents were measured using nanosecond–picosecond two-color two-laser flash photolysis. The fluorescence peaks from  $\text{BPDH}^*(\text{D}_1)$  showed a shift due to the dipole–dipole interaction with the solvent molecules. The dipole moments ( $\mu_e$ ) of  $\text{BPDH}^*(\text{D}_1)$  were estimated to be 7–10 D, indicating that  $\text{BPDH}^*(\text{D}_1)$  are highly polarized. It was revealed that the fluorescence lifetime ( $\tau_f$ ) depends on  $\mu_e$  in acetonitrile because the stabilization by solvent molecules affects the  $\tau_f$  value in polar solvents, predominantly. On the contrary, the conformation of  $\text{BPDH}^*(\text{D}_1)$  plays an important role in cyclohexane because the efficiency of the unimolecular reaction from  $\text{BPDH}^*(\text{D}_1)$  depends on the conformation. The substituent effect on the electron transfer from  $\text{BPDH}^*(\text{D}_1)$  to their parent molecules was also discussed.

## Introduction

Free radicals are one of the most important primary photochemical products. The excited radicals are attractive from the viewpoints of photochemical and photophysical aspects. The radicals in the excited state show two interesting natures.<sup>1</sup> First, it is known that some radicals in the excited state show reactivity different from that in the ground state. Second, a variety of radicals show the characteristic emission from the excited state. The studies on emission from radicals in the excited state will be useful for detecting the radicals in the complicated systems such as biological systems.

Considerable numbers of studies of the excited radicals have been carried out with absorption and emission spectroscopies to elucidate their electronic structures, chemical properties, and reactivities in the condensed phase.<sup>1</sup> Especially, properties of ketyl radicals ( $\text{BPDH}^*$ ) of benzophenone derivatives (BPD) in the excited state ( $\text{BPDH}^*(\text{D}_1)$ ), which show high fluorescence quantum yield (for example, 0.16 for benzophenone ketyl radical ( $\text{BPH}^*$ )), have been investigated vigorously.<sup>1–7</sup> The fluorescence spectra of  $\text{BPDH}^*(\text{D}_1)$  in the condensed phase, gas phase, and polymer matrix were measured using the photochemical and radiolysis techniques.<sup>1–7</sup> The transient absorption spectra of  $\text{BPDH}^*(\text{D}_1)$  were reported by Fessenden et al.<sup>6</sup> In our previous work, we measured absorption spectra of various  $\text{BPDH}^*(\text{D}_1)$  using nanosecond–picosecond two-color two-laser flash photolysis and investigated the substituent effect of  $\text{BPDH}^*(\text{D}_1)$ .<sup>7</sup>

For reactivity,  $\text{BPDH}^*(\text{D}_1)$  showed unique reactions that do not occur from the ground state,<sup>8–11</sup> for example, the O–H bond dissociation to generate the ground-state BPD<sup>8</sup> and electron transfer (ELT) to the ground-state parent molecules from  $\text{BPDH}^*(\text{D}_1)$ .<sup>10,11</sup> Detailed investigation of the reactivity would

develop new techniques using excited radicals. Recently, the efficient fabrication method of gold nanoparticles using the  $\text{BPDH}^*(\text{D}_1)$  as a reducing agent was reported in our laboratory.<sup>12</sup>

The solvent affects the nature and reactivity of molecules in the excited states. Therefore, solvent effects on the properties of open-shell molecules such as radical, radical cation, and radical anion are interesting subjects. However, to the best of our knowledge, there are few reports about the systematic study of solvent effects on the radical in the excited state. Yankov et al. reported the solvent effect on the fluorescence of  $\text{BPH}^*$ .<sup>13</sup> However, the solvent effect on the relaxation processes of  $\text{BPH}^*(\text{D}_1)$  was not revealed due to the poor time resolution of the instruments.

In the present work, we applied nanosecond–picosecond two-color two-laser flash photolysis to measure the absorption and fluorescence spectra of  $\text{BPDH}^*(\text{D}_1)$  in various solvents. These spectroscopic data of  $\text{BPDH}^*(\text{D}_1)$  indicated dipole–dipole interaction with the solvent molecules. The dipole moments of  $\text{BPDH}^*(\text{D}_1)$  ( $\mu_e$ ) were estimated using the Lippert–Mataga treatment. The  $\text{BPDH}^*(\text{D}_1)$  showed high  $\mu_e$  values from 7 to 10 D. The solvent effect on the fluorescence lifetime of  $\text{BPDH}^*(\text{D}_1)$  ( $\tau_f$ ) was also examined. Several factors governing the deactivation processes of  $\text{BPDH}^*(\text{D}_1)$ , such as conformational change in the excited state and bimolecular and unimolecular reactions, were discussed.

## Experimental Section

The two-color two-laser flash photolysis experiment was carried out using the third (355 nm) or fourth (266 nm) harmonic oscillations of a nanosecond  $\text{Nd}^{3+}$ :YAG laser (Quantel, Brilliant; 5 ns fwhm) as the first laser and the second harmonic oscillation (532 nm) of a picosecond  $\text{Nd}^{3+}$ :YAG laser (Continuum, RGA69-10; 30 ps fwhm, 10 Hz) as the second laser. The delay

\* Corresponding author. E-mail: majima@sanken.osaka-u.ac.jp.

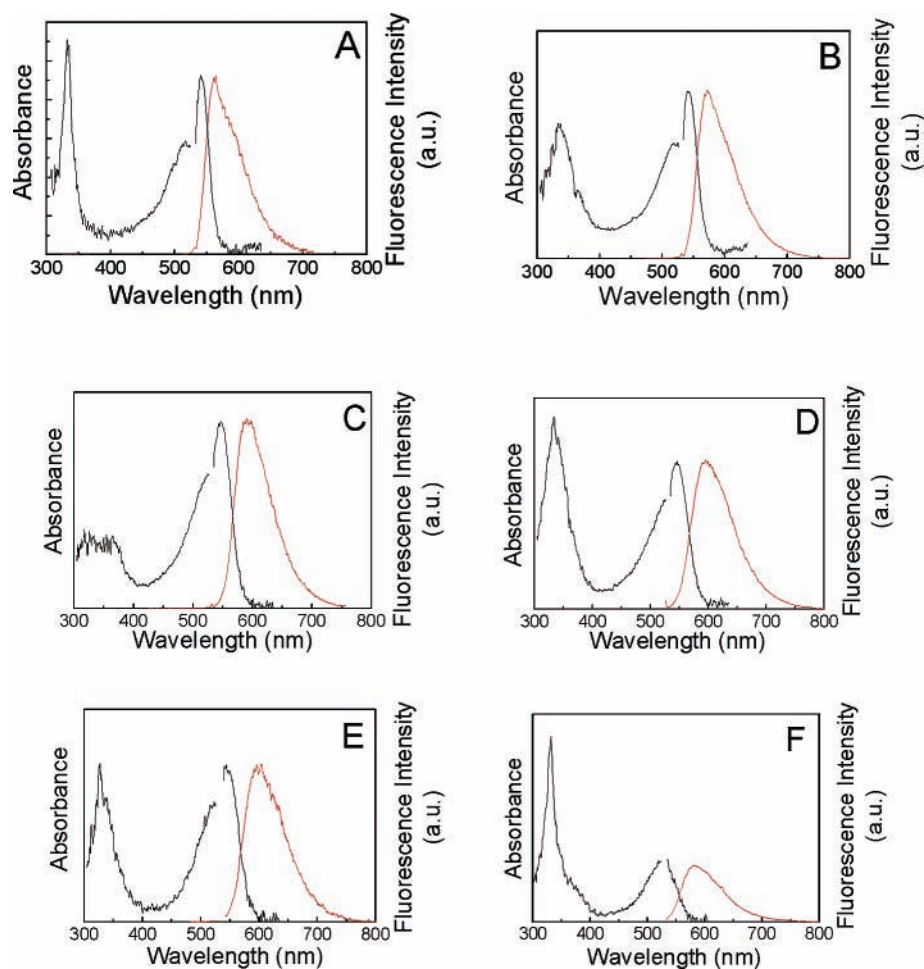


**Figure 1.** Absorption (black line) and fluorescence (red line) spectra of BPH\* in several Ar-saturated solvents at room temperature: Absorption spectra were obtained during the 266 and 532 nm (A, D, E, F) or 355 and 532 nm (B, C) two-color two-laser flash photolysis ((A) cyclohexane; (B) toluene; (C) 2-methyltetrahydrofuran; (D) 2-propanol; (E) methanol; (F) acetonitrile (containing 0.05 M *N,N*-diethylaniline)). The blank around 532 nm in the spectra was due to the residual SHG of Nd<sup>3+</sup>:YAG laser.

time of two laser flashes was adjusted to 1  $\mu$ s by Four Channel Digital Delay/Pulse Generators (Stanford Research Systems, Model DG 535). The breakdown of Xe gas generated by fundamental pulse of the picosecond Nd<sup>3+</sup>:YAG laser was used as a probe light. Transient absorption spectra and kinetic traces were measured using a streak camera (Hamamatsu Photonics, C7700) equipped with a CCD camera (Hamamatsu Photonics, C4742-98) and stored on a personal computer. To avoid stray light and pyrolysis of the sample by the probe light, suitable filters were employed. The samples were flowed in a transparent rectangular quartz cell (1.0  $\times$  0.5  $\times$  2.0 cm) at room temperature.

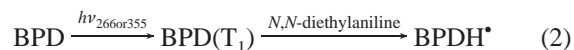
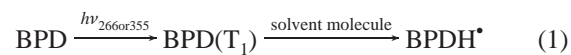
BPD were recrystallized from ethanol before use. Sample solutions were deoxygenated by bubbling Ar gas for 30 min before irradiation.

The dipole moment of BPDH\*(D<sub>0</sub>) ( $\mu_g$ ) and conformation of BPDH\*(D<sub>1</sub>) were calculated at the HF/6-31G\* level.<sup>14</sup> The absorption peaks of the 4,4'-bis(methoxyphenyl)methanol cation and (4-methoxyphenyl)phenylmethanol cation were calculated at the TD/6-311+G(d,p) level.<sup>15</sup>

## Results and Discussion

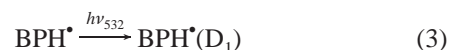
**Generation of BPDH\*.** BPDH\* can be efficiently generated from hydrogen abstraction of BPD in the triplet excited states (BPD(T<sub>1</sub>)) in cyclohexane, toluene, MTHF, and alcohols.<sup>16</sup> BPD(T<sub>1</sub>) decayed through the hydrogen abstraction from hydrogen donor molecules to produce BPDH\* after the first 266 or 355 nm nanosecond-laser irradiation. In cyclohexane, toluene,

MTHF, and alcohols, the solvent itself works as the hydrogen donor molecules (eq 1). In acetonitrile, we used the bimolecular reaction between BPD(T<sub>1</sub>) and *N,N*-diethylaniline to generate BPDH\* efficiently (eq 2).<sup>17</sup>



The absorption spectra of BPH\* in several solvents were shown in Figure 1. These spectra were very consistent with the reported ones.<sup>18</sup> The photophysical data of BPH\* were summarized in Table 1. Absorption peaks of BPH\* in the UV and visible regions have been reported to be the D<sub>2</sub>  $\leftarrow$  D<sub>0</sub> and D<sub>1</sub>  $\leftarrow$  D<sub>0</sub> transitions, respectively.<sup>3</sup> The absorption maxima of BPH\* shifted depending on the solvent properties.

**Fluorescence Spectra of BPH\*.** The generated BPH\* was excited at the visible absorption band using the second laser (532 nm, 12 mJ pulse<sup>-1</sup>, 30 ps fwhm) with the delay time of 1  $\mu$ s after the first laser (eq 3). Upon the excitation, BPH\* showed

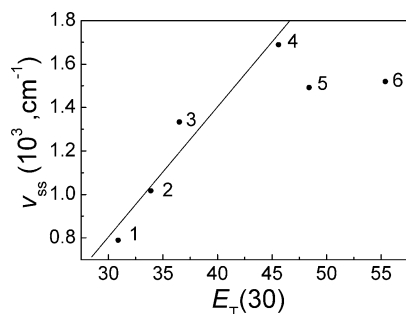


the fluorescence. The fluorescence spectrum of BPH\*(D<sub>1</sub>) was almost a mirror image of the absorption spectrum of BPH\* in

**TABLE 1: Dielectric Constant of Solvent ( $\epsilon$ ) and Data for the Benzophenone Ketyl Radical in Various Solvents**

solvent	$\epsilon$	$\lambda_a^{\max}$ (nm)	$\lambda_f^{\max}$ (nm)	$\lambda_{D_1}^{\max}$ (nm)	$10^{-3}\nu_{SS}$ ( $\text{cm}^{-1}$ )
cyclohexane	2	332, 541	564.9	480	0.79
toluene	2.4	333, <sup>b</sup> 540	571.6	466	1.0
MTHF	7.6	330, <sup>b</sup> 548	590.6	477	1.3
2-propanol	20	334, 547	595.6	481	1.5
methanol	33	327, 544	593.3	463	1.5
acetonitrile <sup>a</sup>	36	331, 530 <sup>c</sup>	582.1	479	1.7

<sup>a</sup> Containing 0.05 M *N,N*-diethylaniline. <sup>b</sup> This value is not clear due to the interference of the ground-state absorption. <sup>c</sup> Error  $\pm 5$  nm due to the residual SHG of Nd<sup>3+</sup>:YAG laser.

**Figure 2.** Plots of Stokes shift values of BPH\* vs  $E_T(30)$ , the solvent polarity parameter: 1, cyclohexane; 2, toluene; 3, MTHF; 4, acetonitrile (containing 0.05 M *N,N*-diethylaniline); 5, 2-propanol; 6, methanol.

each solvent (Figure 1). The fluorescence from BPH\*(D<sub>1</sub>) in cyclohexane with a peak at 565 nm agreed well with the reported one.<sup>2</sup>

The fluorescence spectrum of BPH\* showed a red shift with increasing solvent polarity. The fluorescence maximum of BPH\* and observed Stokes shift ( $\nu_{SS}$ ) in various solvents were listed in Table 1. The shift of the fluorescence peak can be attributed to (1) dipole–dipole interaction between the solvent and solute, (2) changes in the emitting state induced by the solvent, and (3) specific solvent–solute interactions such as hydrogen bonding. To have a better understanding of BPH\* in the excited state, the  $\nu_{SS}$  values were plotted against the Dimroth  $E_T(30)$  parameter.<sup>19</sup> As shown in Figure 2, the  $\nu_{SS}$  values showed a linear correlation with the  $E_T(30)$  parameter except for those in 2-propanol and methanol. Linearity of this plot suggests that the dipole–dipole interaction between solvent and solute is responsible for the solvent-dependent change of the  $\nu_{SS}$  value of BPH\*. Deviation from the line in 2-propanol and methanol indicates that the hydrogen bond formation between the ketyl radical and solvent molecule would not be negligible.

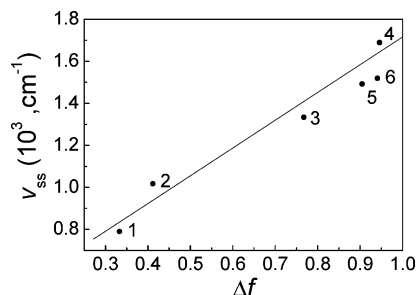
The Lippert–Mataga equation (eq 4) was employed to obtain quantitative information about dipole moment of BPDH\*(D<sub>1</sub>) ( $\mu_e$ ).<sup>20</sup>

$$\nu_{SS} = 2(\mu_e - \mu_g)^2 \Delta f / hca^3 + C \quad (4)$$

where

$$\Delta f = [(\epsilon - 1)/(2\epsilon + 1)] - [(n^2 - 1)/(2n^2 + 1)] \quad (5)$$

In the equations,  $\mu_g$  is the ground-state dipole moment,  $h$  is Planck's constant,  $c$  is the velocity of the light,  $a$  is the radius of the cavity in which the fluorophore resides (Onsager radius) (we assumed that the radius of BPDH\* was 6 Å),  $\Delta f$  is known as the solvent polarity parameter, and  $\epsilon$  and  $n$  are the dielectric constant and refractive index of the medium, respectively. The  $\Delta f$  values for the various solvents were calculated using the

**Figure 3.** Lippert–Mataga plot for BPH\*: 1, cyclohexane; 2, toluene; 3, MTHF; 4, acetonitrile (containing 0.05 M *N,N*-diethylaniline); 5, 2-propanol; 6, methanol.**TABLE 2: Dipole Moment of BPDH\* in the Ground ( $\mu_g$ ) and Excited States ( $\mu_e$ )**

		$\mu_e - \mu_g$ (D)	$\mu_g$ (D)	$\mu_e$ (D)
R	R'			
CF <sub>3</sub>	H	6.6	2.0	8.6
CH <sub>3</sub> O	H	7.6	2.5	10
CH <sub>3</sub> O	CH <sub>3</sub> O	<i>a</i>	<i>a</i>	<i>a</i>
Cl	Cl	6.3	2.1	8.4
Cl	H	5.5	3.7	9.2
Me	Me	6.0	1.8	7.8
Me	H	5.4	1.6	6.9
F	H	6.4	3.2	9.6
F	F	6.7	1.9	8.6
H	H	5.3	1.7	7.0

<sup>a</sup> The value was not determined.

parameters in ref 21. As shown in Figure 3, the  $\nu_{SS}$  values for BPH\* showed a linear relation with  $\Delta f$ . From the slope of the line in the Figure 3, the  $\mu_e - \mu_g$  value of BPH\* was estimated to be 5.3 D. The data points for 2-propanol and methanol were ignored because ketyl radicals and alcohols seem to make a complex due to the formation of hydrogen bonding, as mentioned above. A similar hydrogen bonding complex between BPH\* and triethylamine was reported.<sup>4</sup> The  $\mu_g$  value of BPH\* was calculated at the HF/6-31G\* level. Although this approach assumes that the  $\mu_g$  is independent of solvent and the same as in the gas phase, the effect of solvent–solute interaction to the  $\mu_g$  would be negligible due to the small  $\mu_g$  value. Employing 1.71 D of  $\mu_g$ , the  $\mu_e$  value of BPH\* was calculated to be 7.0 D from the  $\mu_e - \mu_g$  value. The high  $\mu_e$  value indicates that BPH\* was highly polarized in the excited state. The ground- and excited-state dipole moments of BPDH\* were estimated in a similar way as listed in the Table 2.

In the case of the xanthone ketyl radical, the dipole–dipole interaction between the solvent and xanthone ketyl radical in the excited state can be negligible.<sup>22</sup> Therefore, it is suggested that one of the important factors for the large  $\mu_e$  of BPDH\*(D<sub>1</sub>) may be the conformation change in the D<sub>1</sub> state, because the conformation change of the xanthone ketyl radical following the excitation is prevented by the linkage between the two phenyl rings.

The energy gap between the D<sub>1</sub> and D<sub>0</sub> states of BPH\* ( $\Delta E(D_1 - D_0)$ ) in the several solvents was determined from the fluorescence maxima (Table 3). The  $\Delta E(D_1 - D_0)$  value of BPH\*(D<sub>1</sub>) decreased with increasing the solvent polarity. Because the electron distribution of BPH\*(D<sub>1</sub>) was largely polar-



**TABLE 3: Lifetimes of Transient Absorption ( $\tau$ ) and Fluorescence ( $\tau_f$ ), Rate Constant of the Chemical Reaction ( $k_C$ ), Rate Constants of Radiative ( $k_f$ ) and Nonradiative Relaxation Process ( $k_{IC}$ ), and Energy Gap of BPH\* between the D<sub>1</sub> and D<sub>0</sub> States**

solvent	$\tau$ (ns)	$\tau_f$ (ns)	$k_C$ ( $10^8 \text{ s}^{-1}$ )	$k_f + k_{IC}$ ( $10^8 \text{ s}^{-1}$ )	$\Delta E(D_1-D_0)$ (eV)
cyclohexane	$2.0 \pm 0.1^a$	$2.0 \pm 0.1^a$	$1.7 \pm 0.1^a$	$3.4 \pm 0.1^a$	$2.20^a$
toluene	2.8	2.8	<i>c</i>	<i>c</i>	2.17
MTHF	1.8	1.8	<i>c</i>	<i>c</i>	2.10
2-propanol	0.56	0.49	<i>c</i>	<i>c</i>	2.08
methanol	$0.25 \pm 0.02$	$0.26 \pm 0.01$	<i>c</i>	<i>c</i>	2.09
acetonitrile <sup>b</sup>	5	4.7	<i>c</i>	<i>c</i>	2.13

<sup>a</sup> Reference 7. <sup>b</sup> Containing 0.05 M *N,N*-diethylaniline. <sup>c</sup>  $k_C$  and  $k_f + k_{IC}$  values were not determined due to the overlap of generated BPH\*(D<sub>1</sub>) spectra.

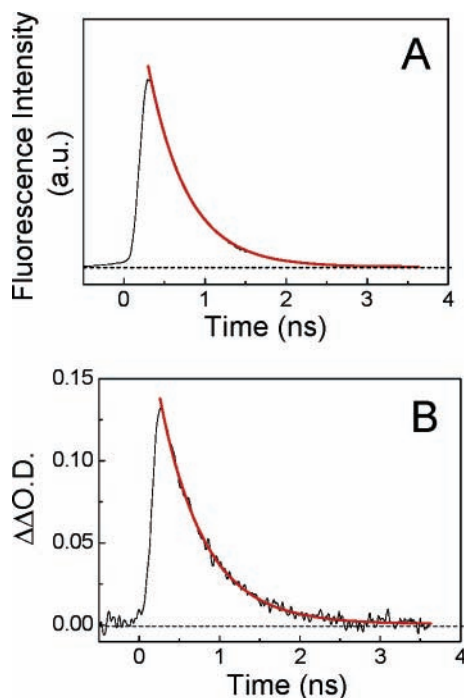


**Figure 4.** Kinetic traces of fluorescence intensity (A) and absorption of BPH\*(D<sub>1</sub>) (B) at 595 and 480 nm, respectively, in 2-propanol during the two-color two-laser photolysis.

ized, it is suggested that BPH\*(D<sub>1</sub>) was stabilized by the dipole–dipole interaction with the solvent molecules. The similar tendency was observed in the cases of the other BPDH\*(D<sub>1</sub>).

**Fluorescence Lifetimes ( $\tau_f$ ) of BPDH\*(D<sub>1</sub>) in Several Solvent.** Fluorescence lifetimes ( $\tau_f$ ) of BPDH\*(D<sub>1</sub>) in each solvent were measured at the peak positions of the fluorescence spectra (see Supporting Information). All fluorescence decay curves were fitted well with the single-exponential decay function (Figure 4). The measured  $\tau_f$  values of BPH\*(D<sub>1</sub>) were 0.5–5 ns (Table 3). In cyclohexane, toluene, and MTHF,  $\tau_f$  values were similar to each other. The  $\tau_f$  values of BPH\*(D<sub>1</sub>) in methanol, which has a polarity similar to acetonitrile's, was the shortest  $\tau_f$  among all solvents used. Additionally, the  $\tau_f$  value was also small in 2-propanol. The shorter  $\tau_f$  in alcohol can be attributed to hydrogen bonding between solute and solvent molecules, which promotes the nonradiative relaxation process.<sup>22,23</sup>

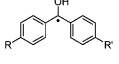
It is remarkable that the solvent effects on the  $\tau_f$  values in acetonitrile were significantly affected by the substituent of BPDH\*(D<sub>1</sub>) (Table 4). In the cases of BPH\*(D<sub>1</sub>), the 4-methylbenzophenone ketyl radical(D<sub>1</sub>), and 4,4'-dimethylbenzophenone ketyl radical(D<sub>1</sub>), the  $\tau_f$  values in acetonitrile were larger

than those in cyclohexane. On the other hand,  $\tau_f$  values of the other BPDH\*(D<sub>1</sub>) in acetonitrile were small compared with those in cyclohexane. These results may be explained as follows. The decay of BPDH\*(D<sub>1</sub>) can be attributed to the combination of inter- and unimolecular chemical reactions and nonradiative and radiative transition processes (Scheme 1). Because BPDH\*(D<sub>1</sub>) were largely polarized as mentioned above, BPDH\*(D<sub>1</sub>) were stabilized by dipole–dipole interaction in polar solvents to decrease  $\Delta E(D_1-D_0)$ . As a result, the nonradiative relaxation process from BPDH\*(D<sub>1</sub>) to BPDH\*(D<sub>0</sub>) was promoted in the polar solvents.<sup>16</sup> BPDH\*(D<sub>1</sub>) with a large  $\mu_e$  value showed the small  $\tau_f$  values in acetonitrile (Figure 5A), supporting the present hypothesis. On the other hand, because the  $\mu_e$  values of BPH\*(D<sub>1</sub>), 4-methylbenzophenone ketyl radical(D<sub>1</sub>), and 4,4'-dimethylbenzophenone ketyl radical(D<sub>1</sub>) were small compared with these of other BPDH\*(D<sub>1</sub>), the excited state was not significantly stabilized by solvent molecules. It is concluded that the  $\tau_f$  values in acetonitrile were largely dependent on the  $\mu_e$  value due to the stabilization by dipole–dipole interaction. Consequently, the above-mentioned effect of substituents on the solvent effect was observed. On the other hand, the  $\mu_e$  value dependence on  $\tau_f$  was not observed in cyclohexane, indicating that the other factor would be predominant in cyclohexane.

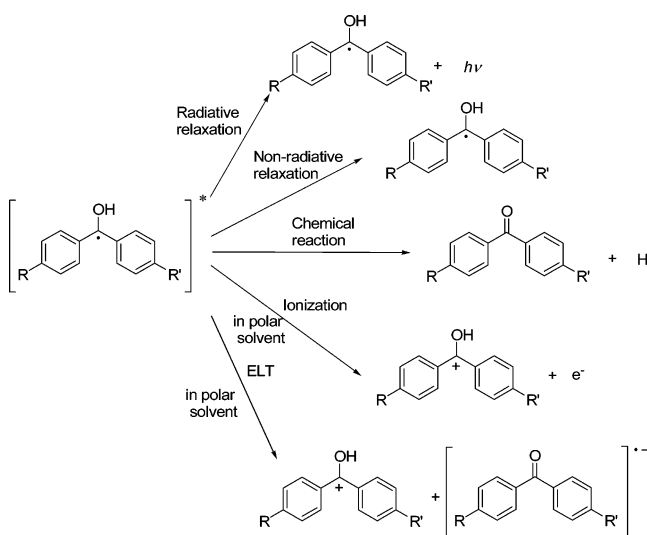
**Decay Processes of BPDH\*(D<sub>1</sub>) in Cyclohexane.** In our previous paper, properties of BPDH\*(D<sub>1</sub>) in cyclohexane were investigated.<sup>7</sup> It was confirmed that  $\tau_f$  in cyclohexane becomes longer with the decreasing  $\nu_{ss}$ . This correlation indicated that conformational change associated with the electronic transition between the D<sub>1</sub> and D<sub>0</sub> states plays an important role in the decay process of BPDH\*(D<sub>1</sub>). Thus, we calculated the conformation of BPDH\*(D<sub>1</sub>) at HF/6-31G\* level to investigate the relation between the conformation and  $\tau_f$ .<sup>14</sup> The optimized conformations of BPH\*(D<sub>0</sub>) and BPH\*(D<sub>1</sub>) were shown in Chart 1. The estimated dihedral angles between the plane containing the benzene ring and that containing the oxygen and hydrogen of the hydroxyl group ( $\Phi_1$  and  $\Phi_2$ ) and angle between the planes containing the benzene rings ( $\gamma$ ) of BPDH\*(D<sub>0</sub>) and BPDH\*(D<sub>1</sub>) were listed in Table 5 (Chart 2). It was revealed that the  $\gamma$  value decreased and that  $\Phi_1$  and  $\Phi_2$  values increased during the excitation. That is, the angle between the planes containing the benzene rings decreased and the twist of two phenyl rings increased during the excitation. It is remarkable that the correlation between the  $\Phi_1 + \Phi_2$  value and  $\tau_f$  values in cyclohexane clearly indicates that the large twist of phenyl rings increases the  $\tau_f$  value (Figure 5B). The  $\tau_f$  values in acetonitrile did not show correlation with the  $\Phi_1 + \Phi_2$  value. Thus, the stabilization by the dipole–dipole interaction would affect the  $\tau_f$  value in acetonitrile, predominantly.

The  $\Phi_1 + \Phi_2$  value dependence on the  $\tau_f$  values in cyclohexane would be explained as follows. The decay of BPDH\*(D<sub>1</sub>) can be attributed to the combination of chemical reactions and nonradiative and radiative transition processes. In cyclohexane, the solvent stabilization effect on BPDH\*(D<sub>1</sub>) should be small. Thus, it is suggested that the decrease of  $\tau_f$  reflects the increase of a chemical reaction process. Because no new transient absorption was observed after the second laser irradiation, the chemical reaction process is the O–H bond cleavage.<sup>8</sup> It is suggested that the extent of charge delocalization relates to the orbital overlap of the  $\pi$  system and nonbonding orbital of oxygen. Consequently, in the case of BPDH\*(D<sub>1</sub>) with small  $\Phi_1 + \Phi_2$  value, the O–H bond cleavage would be promoted due to the orbital overlap. On the contrary, orbital overlap of BPDH\*(D<sub>1</sub>) with a large  $\Phi_1 + \Phi_2$  value should be

**TABLE 4: Reduction Potential of BPD ( $E_{\text{RED}}$ ), Lifetime of BPDH $\cdot$ (D $_1$ ) ( $\tau_f$ ) in Acetonitrile and Cyclohexane, Quenching Rate Constant of BPDH $\cdot$ (D $_1$ ) by *N,N*-Diethylaniline ( $k_q$ ), and Electron Transfer Rate Constant of BPDH $\cdot$ (D $_1$ ) by the Parent Molecules ( $k_{\text{sq}}$ )**

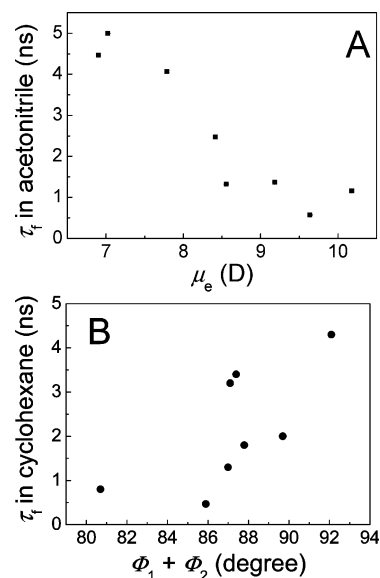
		$E_{\text{RED}}$ (V vs. SCE)	$\tau_f$ (ns) in Acetonitrile	$\tau_f$ (ns) in Cyclohexane	$k_{\text{sq}}$ ( $10^9 \text{ s}^{-1}$ )	$k_{\text{sq}}$ ( $10^{10} \text{ s}^{-1}$ )
R	R'					
CF $_3$	H	-1.58 <sup>a</sup>	1.2	4.3 $\pm$ 0.3	1.1	1.9
CH $_3$ O	H	-1.95 <sup>b</sup>	1.3	0.89	1.9 $\pm$ 0.2	1.5
CH $_3$ O	CH $_3$ O	-2.02 <sup>a</sup>	0.39	0.35	1.6 $\pm$ 0.8	<i>d</i>
Cl	Cl	-1.67 <sup>a</sup>	2.2	3.4 $\pm$ 0.1	1.1	1.3
Cl	H	-1.75 <sup>a</sup>	1.8	3.2 $\pm$ 0.1	1.2	2.2
Me	Me	-1.90 <sup>a</sup>	4.0	1.6	1.3	1.4 $\pm$ 0.3
Me	H	-1.86 <sup>b</sup>	4.4	1.8	1.3	1.9 $\pm$ 0.1
F	H	-1.79 <sup>c</sup>	0.63	1.3 $\pm$ 0.1	1.9	2.1 $\pm$ 0.4
F	F	-1.78	0.24	0.47	1.5 $\pm$ 0.2	<i>d</i>
H	H	-1.83 <sup>a</sup>	4.7	2.0 $\pm$ 0.1	0.99	2.1

<sup>a</sup> Reference 29. <sup>b</sup> Reference 30. The value was corrected by using the  $E_{\text{RED}}$  value of BP. <sup>c</sup> Reference 31. The value was corrected by using the  $E_{\text{RED}}$  value of BP. <sup>d</sup> The value was not estimated due to the low solubility of the parent molecule and short  $\tau_f$ .

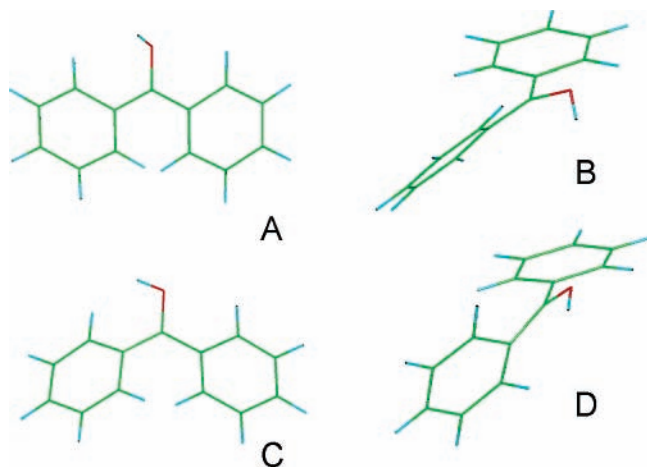
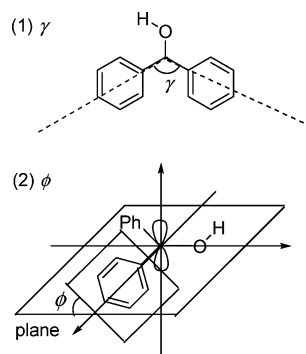
**SCHEME 1**

difficult due to the large twist of phenyl rings. As a result, BPDH $\cdot$ (D $_1$ ) with a large  $\Phi_1 + \Phi_2$  value showed  $\tau_f$  values longer than those of BPDH $\cdot$ (D $_1$ ) with a small  $\Phi_1 + \Phi_2$  value.

**Absorption Spectra of BPH $\cdot$ (D $_1$ ) in 2-Propanol.** Immediately after the second laser irradiation of BPH $\cdot$  in 2-propanol, growth of new transient absorption peaks at around 350 and 480 nm was observed (Figure 6A). Figure 6B is a difference spectrum obtained by subtracting the spectrum observed before the second laser irradiation from that observed at 0.5 ns after the irradiation. From Figure 6, the absorption band due to the  $D_n \leftarrow D_1$  ( $n > 1$ ) transition became apparent. Similar results were obtained in cyclohexane, toluene, MTHF, and methanol. The absorption peak position of BPH $\cdot$ (D $_1$ ) in the visible region was significantly affected by properties of solvent. Although the subtracted spectra do not exhibit the complete transient absorption spectra due to the bleaching of absorption spectra of BPH $\cdot$ (D $_0$ ) upon the second laser excitation, the affect of bleaching on the absorption peak in the visible region was believed to be negligible due to the low  $\Delta\text{OD}$  of BPH $\cdot$ (D $_0$ ) at around 470 nm. The observed absorption peaks ( $\lambda_{D_1}$ ) in the visible region were summarized in Table 1.

**Figure 5.** Plots  $\tau_f$  in acetonitrile vs  $\mu_e$  (A). Plots  $\tau_f$  in cyclohexane vs  $\Phi_1 + \Phi_2$  (B).

**Absorption Spectra of BPDH $\cdot$ (D $_1$ ) in Acetonitrile.** In acetonitrile, a different result was observed after the second laser irradiation. The absorption spectra of 4-methoxybenzophenone ketyl radical before and after irradiation of the second laser were shown in Figure 7A. Immediately after the second laser irradiation, sharp and broad absorption bands appeared at 380 and 420–520 nm, respectively. The broad band centered at ca. 650 nm grew up within 5 ns. Because the lifetime of the broad band at 420–520 nm was 1.2 ns, which is essentially the same as the  $\tau_f$  value, the broad band can be attributed to the 4-methoxybenzophenone ketyl radical(D $_1$ ). The broad band from 580 to 800 nm, which has a long lifetime, was assigned to be the 4-methoxybenzophenone radical anion.<sup>18</sup> The lifetime of the sharp band at 380 nm was  $5.7 \pm 0.4$  ns, which is different from those of the 4-methoxybenzophenone ketyl radical(D $_1$ ) (0.83  $\pm$  0.02 ns) and the 4-methoxybenzophenone radical anion (400 ns). The (4-methoxyphenyl)phenylmethanol cation will be a possible origin of the sharp band. In our previous study, similar absorption of the 4,4'-bis(methoxyphenyl)methanol cation was

**CHART 1: Optimized Conformation of BPH(D<sub>0</sub>) (A and B) and BPH(D<sub>1</sub>) (C and D)****CHART 2**

observed upon the excitation of 4,4'-methoxybenzophenone ketyl radical.<sup>10</sup> Because (4-methoxyphenyl)phenylmethanol cation is expected to deprotonate quickly producing 4-methoxybenzophenone(S<sub>0</sub>),<sup>24</sup> (4-methoxyphenyl)phenylmethanol cation would have a short lifetime compared with 4-methoxybenzophenone radical anion (Scheme 2).

We investigated the nature of the transient species by experimental and theoretical ways. In the presence of tetra-*n*-butylammonium azide (15 mM), the lifetime of the absorption

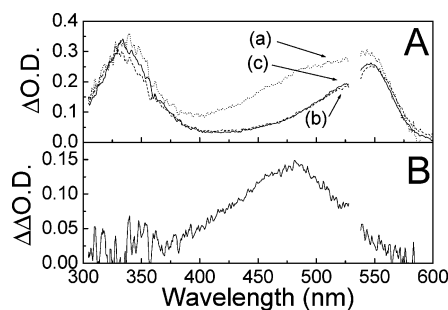


**Figure 6.** Transient absorption spectra observed at 0.5 (dotted line (a)) and 20 ns (broken line (b)) after the second laser irradiation during the two-color two-laser photolysis (266 or 355 and 532 nm), and spectrum during one-laser photolysis (266 nm, solid line (c)) of benzophenone ( $1.0 \times 10^{-4}$  M) (A) in Ar-saturated 2-propanol. The second laser was irradiated at 1  $\mu$ s after the first laser pulse. Transient absorption spectrum of BPH\*(D<sub>1</sub>) (B) was given by subtracting spectrum c from spectrum a. The blank around 532 nm in the spectra was due to the residual SHG of Nd<sup>3+</sup>:YAG laser.

band at 385 nm decreased to 1.6 ns (Figure 7B). The reaction rate of the (4-methoxyphenyl)phenylmethanol cation and tetra-*n*-butylammonium azide was estimated to be  $3.0 \times 10^{10} \text{ M}^{-1} \text{ s}^{-1}$ , which is similar to the diffusion-control rate constant in acetonitrile.<sup>21</sup> Because tetra-*n*-butylammonium azide is a strong nucleophile, the lifetime of the (4-methoxyphenyl)phenylmethanol cation should decrease due to the nucleophilic attack.<sup>25</sup> A similar result was observed in the case of the 4,4'-bis(methoxyphenyl)methanol cation.<sup>10</sup> Furthermore, the absorption bands of the (4-methoxyphenyl)phenylmethanol cation and 4,4'-bis(methoxyphenyl)methanol cation were calculated at the TD/6-311+G-(d,p) level<sup>15</sup> to be 353 and 392 nm, respectively, which are very close to the peaks of the observed absorption spectra. These findings supported our assignment of the transient absorption.

Because the lifetime of the 4,4'-bis(methoxyphenyl)methanol cation (11.3 ns) in acetonitrile was longer than that of the (4-methoxyphenyl)phenylmethanol cation ( $5.7 \pm 0.4$  ns, vide infra) and the 4,4'-bis(methylphenyl)methanol cation ( $3.8 \pm 0.8$  ns, vide infra), it is suggested that the electron donating group stabilizes the cation and decreases the deprotonation rate.

In the case of the 4,4'-dimethylbenzophenone ketyl radical, the absorption tail of the cation was observed upon the second laser irradiation. For other BPDH\*, corresponding cations were

**TABLE 5: Dihedral Angles between the Plane Containing the Benzene Ring and That Containing the Oxygen and Hydrogen of the Hydroxyl Group of BPDH\*(D<sub>0</sub>) and BPDH\*(D<sub>1</sub>) ( $\Phi_1(g)$ ,  $\Phi_2(g)$ ,  $\Phi_1(e)$ , and  $\Phi_2(e)$ , Respectively), Angle between the Planes Containing the Benzene Rings of BPDH\*(D<sub>0</sub>) and BPDH\*(D<sub>1</sub>) ( $\gamma(g)$  and  $\gamma(e)$ , Respectively)**

		$\gamma(e)$	$\phi_1(e)$	$\phi_2(e)$	$\gamma(g)$	$\phi_1(g)$	$\phi_2(g)$
R	R'	degree	degree	degree	degree	degree	degree
CF <sub>3</sub>	H	126.2	58.6	33.5	128	19.4	22.8
CH <sub>3</sub> O	H	126.2	47.4	33.3	128.2	18	24.5
CH <sub>3</sub> O	CH <sub>3</sub> O	<i>a</i>	<i>a</i>	<i>a</i>	<i>a</i>	<i>a</i>	<i>a</i>
Cl	Cl	125.9	51.8	35.6	128	18.5	23.7
Cl	H	128.1	49.8	37.3	128.1	17.8	24.5
Me	Me	<i>a</i>	<i>a</i>	<i>a</i>	<i>a</i>	<i>a</i>	<i>a</i>
Me	H	126.1	52.8	35	128.2	18.2	23.6
F	H	126	51.6	35.4	128.1	18.6	23.7
F	F	126	51.1	34.8	128.1	18.7	24
H	H	126.1	56.1	36.1	128.2	18.5	23.8

<sup>a</sup> The value was not calculated.

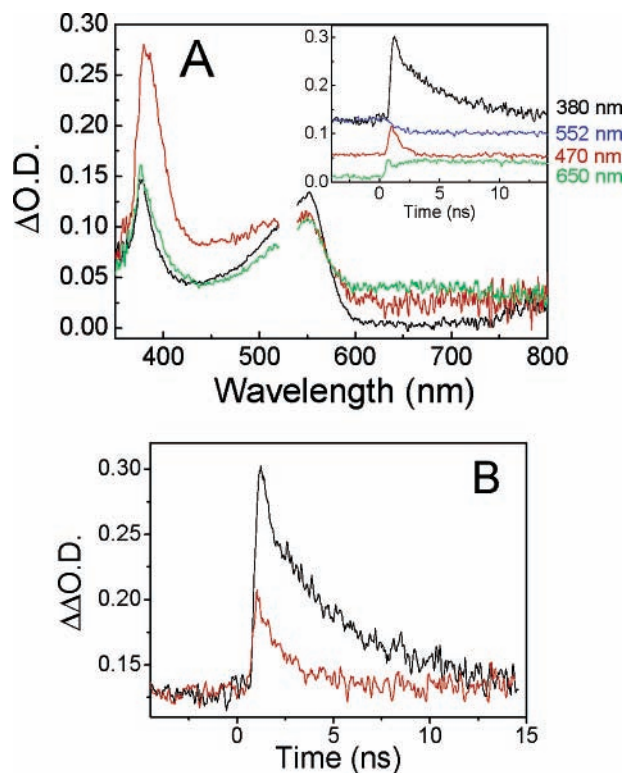
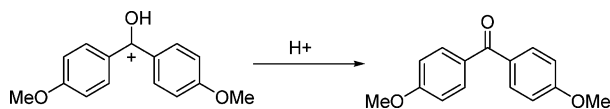
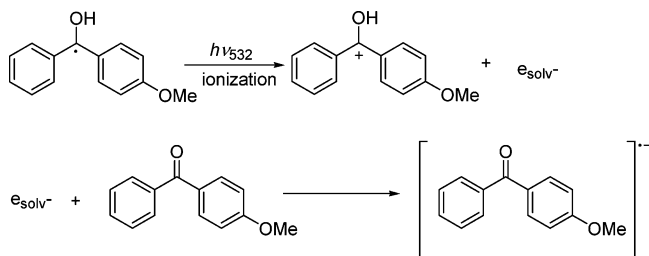


**Figure 7.** Transient absorption spectra observed at 1 (red line) and 10 ns (green line) after the second laser irradiation during the two-color two-laser photolysis (355 and 532 nm), and spectrum during one-laser photolysis (black line) of 4-methoxybenzophenone ( $1.0 \times 10^{-2}$  M) in Ar-saturated acetonitrile. The inset shows the time profiles during the two-color two-laser flash photolysis (A). The time profile at 380 nm in the presence (red line) and absence (black line) of tetra-*n*-butylammonium azide (15 mM) (B).

#### SCHEME 2



#### SCHEME 3



not observed during the 532 nm laser excitation. It is suggested their cations have absorption in the wavelength region shorter than that of the (4-methoxyphenyl)phenylmethanol cation because the electron donating substituents of the (4-methoxyphenyl)phenylmethanol cation could stabilize the cation and cause a red shift of the absorption band. The red shift of the absorption peaks of the 4,4'-bis(methylphenyl)methanol cation ( $<370$  nm) and the (4-methoxyphenyl)phenylmethanol cation (380 nm) compared with that of the 4,4'-bis(methoxyphenyl)methanol cation (400 nm) supports the hypothesis.<sup>10</sup>

**Electron Transfer from BPDH•(D<sub>1</sub>) to BPD(S<sub>0</sub>).** For the formation process of the cation and radical anion after the second laser irradiation, there are two possible pathways. *Pathway I* involves the ionization of BPDH• following the injection of an

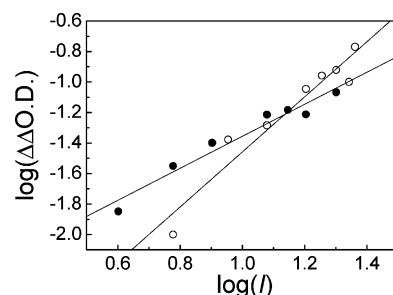


**Figure 8.** Log–log plots of ionization of the 4-methoxybenzophenone ketyl radical ( $\log(\Delta\Delta OD_{380})$  vs  $\log(I)$  (○)) and the 4,4'-dimethoxybenzophenone ketyl radical ( $\log(\Delta\Delta OD_{400})$  vs  $\log(I)$  (●)) in acetonitrile.

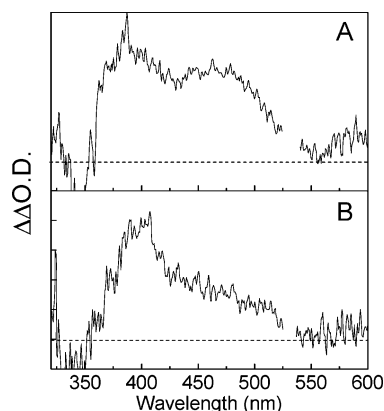


**Figure 9.** Transient absorption spectrum of the 4-methoxybenzophenone ketyl radical(D<sub>1</sub>) (A) and the 4,4'-dimethoxybenzophenone ketyl radical(D<sub>1</sub>) (B) in cyclohexane given by subtracting the spectrum before and 5 ns after the excitation of the second laser. The blank around 532 nm in the spectra was due to the residual SHG of Nd<sup>3+</sup>:YAG laser.

electron to the solvent. Scaiano et al. reported that BPH• was ionized upon the excitation to inject an electron to the solvent. The solvated electron ( $e_{solv-}$ ) was quickly trapped by the ground-state benzophenone to produce the benzophenone radical anion. It is suggested that the cation and radical anion were generated from the similar stepwise reaction process (Scheme 3).

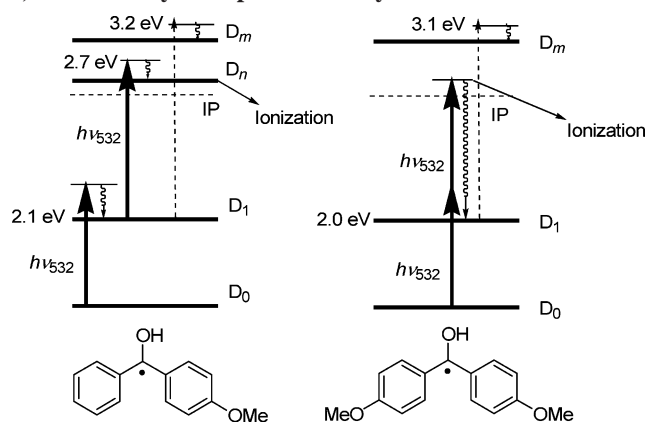
To elucidate the ionization mechanism of the 4-methoxybenzophenone ketyl radical, the laser power ( $I$  in  $\text{mJ pulse}^{-1}$ ) dependence of the ionization yield was investigated. Plots of  $\log(\Delta OD_{380})$  vs  $\log(I)$  showed the linear correlation with a slope of 0.99 at the laser fluence of 4–20  $\text{mJ pulse}^{-1}$  in acetonitrile (Figure 8). On the other hand, in the case of ionization of the 4,4'-dimethoxybenzophenone ketyl radical, the slope of the log–log plot was estimated to be 2. The difference of slopes was explained as follows.

Allonas et al. estimated the adiabatic ionization potential (IP) of the benzophenone ketyl radical to be 5.94 eV by the theoretical calculation at the B3LYP/6-31+G(d) level.<sup>26</sup> Because one-photon absorption of 532 nm light does not give enough energy for ionization, the ionization should occur by the multiphoton process. In the previous work, the ionization process of the 4,4'-dimethoxybenzophenone ketyl radical was revealed to be two-photon process. It is suggested that the 4-methoxybenzophenone ketyl radical is also ionized via a two-photon process.

The spectral shape of the 4,4'-dimethoxybenzophenone ketyl radical(D<sub>1</sub>) and the 4-methoxybenzophenone ketyl radical(D<sub>1</sub>) given by subtracting the spectrum observed before the second laser irradiation were shown in Figure 9. The 4-methoxybenzophenone ketyl radical(D<sub>1</sub>) showed the absorption peak at the visible region, indicating that the second laser with high photon density excites both the D<sub>0</sub> and D<sub>1</sub> states. In this case, stepwise



**SCHEME 4: Ionization Process of the 4-Methoxybenzophenone Ketyl Radical and the 4,4'-Dimethoxybenzophenone Ketyl Radical**



two-photon absorption of the 4-methoxybenzophenone ketyl radical occurs within the second laser pulse. That is, upon excitation with the second laser, most of the 4-methoxybenzophenone ketyl radical ( $D_0$ ) was excited to be 4-methoxybenzophenone ketyl radical ( $D_1$ ); the 4-methoxybenzophenone ketyl radical ( $D_1$ ) absorbed the second photon within the second laser pulse to generate the 4-methoxybenzophenone ketyl radical ( $D_n$  ( $n > 2$ )).

The vertical energy of the 4-methoxybenzophenone ketyl radical ( $D_n$ ) was roughly estimated to be around 5.7 eV. Because the substitution of the electron donating substituent and solvation by the polar solvent decrease the IP, the experimental IP value of the 4-methoxybenzophenone ketyl radical was expected to be smaller than the theoretical value. The vertical energy of the 4-methoxybenzophenone ketyl radical ( $D_n$ ) would be higher than the IP. The ionization would occur from the 4-methoxybenzophenone ketyl radical ( $D_n$ ) (Scheme 4). Because the above-mentioned stepwise two-photon absorption process was considered as a one-photon process, the slopes of plots in Figure 8 were close to 1. A similar result was reported by Miyasaka et al. for the photochromic process of diarylethene using the picosecond laser.<sup>27</sup> In contrast, in the case of the 4,4'-dimethoxybenzophenone ketyl radical, the  $D_1$  state showed a weak shoulder at the visible region and the second laser would not excite the absorption of the 4,4'-dimethoxybenzophenone ketyl radical ( $D_1$ ). The ionization would occur via the simultaneous two-photon process (Scheme 4). In such a case, the slope of the plots in Figure 8 became 2.

*Pathway II* is a self-quenching-like ELT from  $BPDH^*(D_1)$  to  $BPD(S_0)$  to give cation and radical anion (Scheme 1). In our previous papers, we found the ELT from the 4,4'-dimethoxybenzophenone ketyl radical ( $D_1$ ) and  $BPH^*(D_1)$  to those parent molecules.<sup>10,11</sup> In the present study, it was confirmed that the  $\tau_f$  of  $BPDH^*(D_1)$  in acetonitrile decreased with increasing concentration of parent molecules. Because  $BPDH^*(D_0)$  has quite a low oxidation potential (for example,  $E_{OX} = -0.25$  V vs SCE for  $BPH^*(D_0)$ ),<sup>28</sup> the ELT from  $BPDH^*(D_1)$  to  $BPD(S_0)$  is possible. Furthermore, in the case of 4-methoxybenzophenone ketyl radical ( $D_1$ ), the ELT process was also confirmed by the growth of the 4-methoxybenzophenone radical anion. Because the growth rate of the 4-methoxybenzophenone radical anion is similar to the decay rate of the fluorescence, it is indicated that the ELT from the 4-methoxybenzophenone ketyl radical ( $D_1$ ) to the parent molecules generates the radical anion (Figure 7A). A similar ELT process was confirmed for other  $BPDH^*$ .

In the present study, we examined the substituent effect on the ELT from  $BPDH^*(D_1)$  to the parent molecules. The

quenching of  $BPDH^*(D_1)$  by  $BPD(S_0)$  was observed for all present  $BPDH^*$  except for the 4,4'-dimethoxybenzophenone ketyl radical ( $D_1$ ) and the 4,4'-fluorobenzophenone ketyl radical ( $D_1$ ). The quenching process of the 4,4'-dimethoxybenzophenone ketyl radical ( $D_1$ ) and the 4,4'-fluorobenzophenone ketyl radical ( $D_1$ ) could not be investigated due to the low solubility. It is indicated that both ELT *pathways I* and *II* occur upon the second laser excitation of the  $BPDH^*(D_0)$ . The bimolecular reaction rate constants of the ELT between  $BPDH^*(D_1)$  and  $BPD(S_0)$  was estimated by using the Stern–Volmer analysis. Because 4-methoxybenzophenone ( $T_1$ ) has quite a low hydrogen abstraction ability in polar solvent, we employed bimolecular reaction between  $BPD(T_1)$  and *N,N*-diethylaniline to form  $BPDH^*(D_1)$  (vide supra). Although the experiment was carried out in the presence of several concentrations of *N,N*-diethylaniline, the shape of the fluorescence spectrum was not changed. Thus, it is concluded that the interaction between  $BPDH^*(D_1)$  and aniline can be neglected under the present experimental conditions. A similar experimental result was reported by Obi et al. in the  $BPH^*(D_0)$ –triethylamine system.<sup>4</sup> They reported that  $BPH^*(D_0)$  forms the nonemissive complex with triethylamine due to the hydrogen bond formation, and the fluorescence was derived from free  $BPH^*(D_0)$ .

It is reported that  $BPDH^*(D_1)$  is reactive with *N,N*-diethylaniline. Thus, the intrinsic fluorescence lifetime ( $\tau_{f0}$ ) was estimated from the linear correlation between  $1/\tau_f$  vs concentration of *N,N*-diethylaniline ( $[N,N\text{-diethylaniline}]$ ) and  $1/\tau_f$  vs concentration of parent molecules ( $[S_0]$ ) according to eq 6,<sup>16</sup> where  $k_q$

$$\frac{1}{\tau_f} = \frac{1}{\tau_{f0}} + k_{sq}[S_0] + k_q[N,N\text{-diethylaniline}] \quad (6)$$

and  $k_{sq}$  denote the bimolecular reaction rate constants for the reaction of  $BPDH^*(D_1)$  with *N,N*-diethylaniline and the parent molecule, respectively.

The  $k_q$  and  $k_{sq}$  values of  $BPDH^*(D_1)$  were estimated and summarized in Table 4. The  $k_q$  values of  $BPDH^*(D_1)$  were  $(1-2) \times 10^9 \text{ M}^{-1} \text{ s}^{-1}$ . On the other hand, almost all  $k_{sq}$  values of  $BPDH^*(D_1)$  were similar to the diffusion-controlled rate constant in acetonitrile.<sup>21</sup>

The reduction potentials ( $E_{RED}$ ) of  $BPD$  were also shown in Table 4. It seems that the ELT to  $BPD$  with small  $E_{RED}$  shows small  $k_{sq}$  value. According to the Rehm–Weller equation, the driving force of ELT increases with increasing  $E_{RED}$ . It is suggested that the  $k_{sq}$  value increased because of the large driving force due to large  $E_{RED}$  value. Although  $E_{RED}$  of 4-methoxybenzophenone ( $S_0$ ) ( $E_{RED} = -1.95$  V)<sup>28</sup> is smaller than those of other  $BPD(S_0)$ , the efficient ELT was observed. It is suggested that the reducing power of  $BPDH^*(D_1)$  was quite high, and sufficient driving force was obtained.

## Conclusions

In the present study, the absorption and fluorescence spectra of  $BPDH^*(D_1)$  were measured in various solvents.  $BPDH^*(D_1)$  showed a dipole–dipole interaction with the solvent molecules. The  $\mu_e$  values were obtained from Lippert–Mataga treatment.  $BPDH^*(D_1)$  showed high  $\mu_e$  values from 7 to 10 D, indicating that  $BPDH^*(D_1)$  were highly polarized. It was revealed that  $\tau_f$  values depend on  $\mu_e$  in acetonitrile due to the stabilization of solvent. On the contrary, the conformation of  $BPDH^*(D_1)$  plays an important role in cyclohexane because the O–H bond cleavage of  $BPDH^*(D_1)$  depends on the conformation. The electron transfer from  $BPDH^*(D_1)$  to their parent molecules was



observed. Because  $E_{\text{OX}}$  of BPDH\* was quite high, the sufficient driving force was obtained regardless of the small  $E_{\text{RED}}$  value.

**Acknowledgment.** We thank Prof. K. Yamaguchi and Dr. Y. Kitagawa for discussions about the theoretical calculation of excited radicals. This work has been partly supported by a Grant-in-Aid for Scientific Research (Project 17105005, Priority Area (417), 21st Century COE Research, and others) from the Ministry of Education, Culture, Sports, Science and Technology (MEXT) of the Japanese Government.

**Supporting Information Available:**  $\tau_f$  of BPDH\*(D<sub>1</sub>) in several solvents. This material is available free of charge via the Internet at <http://pubs.acs.org>.

## References and Notes

- (1) (a) Ramamurthy, V.; Schanze, K. S. *Molecular and supramolecular photochemistry*; Marcel Dekker: New York, 1994; Vol 2. (b) Scaiano, J. C.; Johnston, L. J.; McGimpsey, W. G.; Weir, D. *Acc. Chem. Res.* **1988**, *21*, 22. (c) Melnikov, M. Y.; Smirnov, V. A. *Handbook of Photochemistry of Organic Radicals*; Begell House: New York, 1996.
- (2) (a) Hodgson, B. W.; Keene, J. P.; Land, E. J.; Swallow, A. J. *J. Chem. Phys.* **1975**, *63*, 3671. (b) Topp, M. R. *Chem. Phys. Lett.* **1976**, *39*, 423. (c) Razi Naqvi, K.; Wild, U. P. *Chem. Phys. Lett.* **1976**, *41*, 570. (d) Obi, K.; Yamaguchi, H. *Chem. Phys. Lett.* **1978**, *54*, 448. (e) Baumann, H.; Schumacher, K. P.; Timpe, H.-J.; Řehák, V. *Chem. Phys. Lett.* **1982**, *89*, 315. (f) Hiratsuka, H.; Yamazaki, T.; Maekawa, Y.; Hikida, T.; Mori, Y. *J. Phys. Chem.* **1986**, *90*, 774.
- (3) Thurnauer, M. C.; Meisel, D. *Chem. Phys. Lett.* **1982**, *92*, 343.
- (4) (a) Kajii, Y.; Itabashi, H.; Shibuya, K.; Obi, K. *J. Phys. Chem.* **1992**, *96*, 7244. (b) Wada, S.; Matsushita, Y.; Obi, K. *J. Phys. Chem. A* **1997**, *101*, 2423.
- (5) Hamatani, S.; Tsuji, K.; Kawai, A.; Shibuya, K. *Phys. Chem. Chem. Phys.* **2003**, *5*, 1370.
- (6) Nagarajan, V.; Fessenden, R. W. *Chem. Phys. Lett.* **1984**, *112*, 207.
- (7) Sakamoto, M.; Cai, X.; Hara, M.; Tojo, S.; Fujitsuka, M.; Majima, T. *J. Phys. Chem. A* **2004**, *108*, 8147.
- (8) Johnston, L. J.; Loughnot, D. J.; Wintgens, V.; Scaiano, J. C. *J. Am. Chem. Soc.* **1988**, *110*, 518.
- (9) (a) Baumann, H.; Merckel, C.; Timpe, H.-J.; Graness, A.; Kleinschmidt, J.; Gould, I. R. Turro, N. J. *Chem. Phys. Lett.* **1984**, *103*, 497. (b) Redmond, R. W.; Scaiano, J. C.; Johnston, L. J. *J. Am. Chem. Soc.* **1992**, *114*, 9768. (c) Scaiano, J. C.; Tanner, M.; Weir, D. *J. Am. Chem. Soc.* **1985**, *107*, 4396. (d) Johnston, L. J.; Scaiano, J. C. *J. Am. Chem. Soc.* **1985**, *107*, 6368. (e) Adam, W.; Kita, F.; Oestrich, R. F. *J. Photochem. Photobiol. A* **1994**, *80*, 187.
- (10) Sakamoto, M.; Cai, X.; Hara, M.; Tojo, S.; Fujitsuka, M.; Majima, T. *J. Phys. Chem. A* **2005**, *109*, 6830.
- (11) Sakamoto, M.; Cai, X.; Hara, M.; Tojo, S.; Fujitsuka, M.; Majima, T. *Chem. Eur. J.* **2006**, *12*, 1610.
- (12) Sakamoto, M.; Tachikawa, T.; Fujitsuka, M.; Majima, T. *Chem. Phys. Lett.* **2006**, *420*, 90.
- (13) Yankov, P.; Nickolov, Z.; Zhelyaskov, V.; Petokov, I. *J. Photochem. Photobiol. A* **1989**, *47*, 155.
- (14) Calculation was performed using Spartan02, Wavefunction, Inc., 18401 Von Karman Avenue, Suite 370, Irvine, CA 92612.
- (15) Frisch, M. J.; Trucks, G. W.; Schlegel, H. B.; Scuseria, G. E.; Robb, M. A.; Cheeseman, J. R.; Montgomery, J. A., Jr.; Vreven, T.; Kudin, K. N.; Burant, J. C.; Millam, J. M.; Iyengar, S. S.; Tomasi, J.; Barone, V.; Mennucci, B.; Cossi, M.; Scalmani, G.; Rega, N.; Petersson, G. A.; Nakatsuji, H.; Hada, M.; Ehara, M.; Toyota, K.; Fukuda, R.; Hasegawa, J.; Ishida, M.; Nakajima, T.; Honda, Y.; Kitao, O.; Nakai, H.; Klene, M.; Li, X.; Knox, J. E.; Hratchian, H. P.; Cross, J. B.; Bakken, V.; Adamo, C.; Jaramillo, J.; Gomperts, R.; Stratmann, R. E.; Yazyev, O.; Austin, A. J.; Cammi, R.; Pomelli, C.; Ochterski, J. W.; Ayala, P. Y.; Morokuma, K.; Voth, G. A.; Salvador, P.; Dannenberg, J. J.; Zakrzewski, V. G.; Dapprich, S.; Daniels, A. D.; Strain, M. C.; Farkas, O.; Malick, D. K.; Rabuck, A. D.; Raghavachari, K.; Foresman, J. B.; Ortiz, J. V.; Cui, Q.; Baboul, A. G.; Clifford, S.; Cioslowski, J.; Stefanov, B. B.; Liu, G.; Liashenko, A.; Piskorz, P.; Komaromi, I.; Martin, R. L.; Fox, D. J.; Keith, T.; Al-Laham, M. A.; Peng, C. Y.; Nanayakkara, A.; Challacombe, M.; Gill, P. M. W.; Johnson, B.; Chen, W.; Wong, M. W.; Gonzalez, C.; Pople, J. A. *Gaussian 03*, revision C.02; Gaussian, Inc.: Wallingford, CT, 2004.
- (16) (a) *Modern Molecular Photochemistry*; Turro, N. J., Ed.; Benjamin/Cummings Publishing Co.: Menlo Park, CA, 1978. (b) Suppan, P. *Chemistry and light*; The Royal Society of Chemistry: Cambridge, U.K., 1994.
- (17) (a) Matsushita, Y.; Kajii, Y.; Obi, K. *J. Phys. Chem.* **1992**, *96*, 4455. (b) Arimitsu, S.; Masuhara, H.; Mataga, N.; Tsubomura, H. *J. Phys. Chem.* **1975**, *79*, 1255. (c) Simon, J. D.; Peters, K. S. *J. Am. Chem. Soc.* **1983**, *105*, 4875. (d) Miyasaka, H.; Morita, K.; Kamada, K.; Mataga, N. *Chem. Phys. Lett.* **1991**, *178*, 504. (e) Miyasaka, H.; Morita, K.; Kamada, K.; Nagata, T.; Kiri, M.; Mataga, N. *Bull. Chem. Soc. Jpn.* **1991**, *64*, 3229. (f) Peters, K. S.; Kim, G. *J. Phys. Chem. A* **2004**, *108*, 2598.
- (18) Shida, T. *Electronic absorption spectra of radical ions (Physical Science Data 34)*; Elsevier: Amsterdam, 1988.
- (19) Reichardt, C. *Chem. Rev.* **1994**, *94*, 2319.
- (20) (a) Lippert, E. Z. *Naturforsch.* **1955**, *10a*, 541. (b) Mataga, N.; Kaifu, Y.; Koizumi, M. *Bull. Chem. Soc. Jpn.* **1956**, *29*, 465.
- (21) (a) Murov, S. L.; Carmichael, I.; Hug, G. L. *Handbook of Photochemistry*, 2nd ed; Marcel Dekker: New York, 1993. (b) Riddick, J. A.; Bunger, W. B.; Sakano, T. K. *Techniques of Chemistry*, 4th ed; John Wiley and Sons: Canada, 1986; Vol. 2.
- (22) Sakamoto, M.; Cai, X.; Hara, M.; Tojo, S.; Fujitsuka, M.; Majima, T. *J. Phys. Chem. A* **2005**, *109*, 2452.
- (23) (a) Biczók, L.; Bérces, T.; Linschitz, H. *J. Am. Chem. Soc.* **1997**, *119*, 11071. (b) Biczók, L.; Bérces, T.; Inoue, H. *J. Phys. Chem. A* **1999**, *103*, 3837.
- (24) (a) Bietti, M.; Lanzalunga, O. *J. Org. Chem.* **2002**, *67*, 2632. (b) Baciocchi, E.; Bietti, M.; Steenken, S. *Chem. Eur. J.* **1999**, *5*, 1785. (c) Baciocchi, E.; Belvedere, S.; Bietti, M.; Lanzalunga, O. *Eur. J. Org. Chem.* **1998**, *1*, 299.
- (25) (a) Johnston, L. J.; Lobaugh, J.; Wintgens, V. *J. Phys. Chem.* **1989**, *93*, 7370. (b) Alonso, E. O.; Johnston, L. J.; Scaiano, J. C.; Toscano, V. G. *J. Am. Chem. Soc.* **1990**, *112*, 1270. (c) McClelland, R. A.; Kanagasabapathy, V. M.; Banait, N. S.; Steenken, S. *J. Am. Chem. Soc.* **1991**, *113*, 1009. (d) Faria, J. L.; Steenken, S. *J. Phys. Chem.* **1992**, *96*, 10869. (e) Davidse, P. A.; Kahley, M. J.; McClelland, R. A.; Novak, M. *J. Am. Chem. Soc.* **1994**, *116*, 4513. (f) Pohlert, G.; Scaiano, J. C.; Step, E.; Sinta, R. *J. Am. Chem. Soc.* **1999**, *121*, 6167. (g) Shukla, D.; Lu, C.; Schepp, N. P.; Bentrude, W. G.; Johnston, L. J. *J. Org. Chem.* **2000**, *65*, 6167.
- (26) Lalevé, J.; Allonas, X.; Fouassier, J. *J. Phys. Chem. A* **2004**, *108*, 4326–4334.
- (27) Miyasaka, H.; Murakami, M.; Itaya, A.; Guillaumont, D.; Nakamura, S.; Irie, M. *J. Am. Chem. Soc.* **2001**, *123*, 753.
- (28) Lund, T.; Wayner, D. D. M.; Jonsson, M.; Larsen, A. G.; Daasbjerg, K. *J. Am. Chem. Soc.* **2001**, *123*, 12590.
- (29) Wagner, P. J.; Truman, R. J.; Puchalski, A. E.; Wake, R. *J. Am. Chem. Soc.* **1986**, *108*, 1127.
- (30) Bewick, A.; Jones, V. W.; Karaji, M. *Electrochim. Acta* **1996**, *41*, 1961.
- (31) Leigh, W. J.; Arnold, D. R.; Baines, K. M. *Tetrahedron Lett.* **1981**, *22*, 909.